SSRG International Journal of Civil Engineering
ISSN: 2348-8352/ https://doi.org/10.14445/23488352/IJCE-V11I11P113

Volume 11 Issue 11, 145-152, November 2024

Original Article

Experimental and Numerical Investigation of Geosynthetic Reinforced Concrete Structure

R. Xavier[1], K. Mukilan[2]

[1,2]*Department of Civil Engineering, Kalasalingam Academy of Research and Education, Tamil Nadu, India.*

[1]*Corresponding Author : xaviercivil08@gmail.com*

Received: 11 August 2024 Revised: 09 September 2024 Accepted: 10 October 2024 Published: 30 November 2024

Abstract *- In addition to enhancing soil, geogrids of geosynthetic materials are beneficial for stabilizing and strengthening applications in infrastructure. Biaxial Geogrids (BG) are utilized in the most important experimental study of a Geosynthetic Reinforced Concrete Structure (GRCS) to replace conventional transverse steel reinforcement in structures. Laboratory testing was done on the fill material, geogrid, and foundation soil. A saturated soft foundation layer has supported the concrete structures. During constructing the GRCS in the mud soil, the geogrids' strain values were measured and registered. Based on the test results, the GRCS's construction produced more than fifty percent of the pressure in the geogrids, despite the bulk of the strain being encased in the ground. Internal geogrid confinement thus provides an efficient method for increasing the GRCS's ductility and load carrying ability. Because geogrid has wonderful ductile behavior, it can be utilized as a hybrid reinforcement with a conventional steel bar to enhance building seismic performance, making them more durable and requiring less construction effort. By implementing geo-synthetic reinforced concrete, the models accurately predicted the stress-strain response. An examination of the building expenses concludes that the cost of a typical reinforced concrete structure can reach up to four times that of a GRCS using optimal design.*

Keywords *- Geosynthetics, Soft foundation layer, Numerical modeling, Field instrumentation, Geosynthetic Reinforced Concrete Structure (GRCS), Seismic performance.*

1. Introduction

Despite their straightforward and inexpensive construction, Geosynthetic Reinforced Concrete Structures (GRCS) function well under static and dynamic loading. Geo-synthetic material is the term used to refer to the various types of synthetic material used in civil and environmental construction and other construction applications, such as associated geotextiles, geomembranes and geogrids. GRCS created nearby rivers and streams that were susceptible to scour and water flow. Nonetheless, this can be prevented via various countermeasures [1-2]. However, GRCS's cost-effectiveness may be diminished by implementing excessively pricey countermeasures; for these reasons, alternative approaches should be considered [3].

This paper examined an embedded GRCS with an appropriate offset from the stream to prevent scouring. Reinforced concrete columns comprise one of the structural elements believed to be particularly prone to failure to unpredictable impact loads, including blast loads or earthquakes. When beams fail, the buildings they maintain sometimes collapse seriously [4-5]. A building constructed using Reinforced Concrete (R/C) plays an important role in ensuring that columns and other corresponding reinforcement components behave ductility. Because stirrups and different kinds of fibers can affect the R/C members' flexural and shear capabilities, many studies have been done to evaluate how they affect [6].

In order to lower inertial forces, save costs, and increase durability, a significant amount of research has also been done on developing original, smart materials that possess significant strength, low weight, and increased ductility. The primary goal of this research is to the real-world usage of geogrids. This geosynthetic material has become increasingly popular in construction enterprises, particularly infrastructure. The expense objective capability, the cheapest plan, happens by assuming a bunch of natural and plan contemplations that concur with current practice guidelines [7].

The stress levels in the land networks have been estimated and recorded both during the projection development stage and after the scaffold's structure was finished, following the selection of the most appropriate GRCS design for an unstructured reinforced bridge in this instance. Geogrid is a geosynthetic material with a grid form specializing in soil stabilization. The fill material and foundation soil were investigated in laboratories [8-9]. The outcomes of a FEM

computational investigation were compared with the actual geogrid strains determined using strain gauges for the full-scale GRCS. It should be highlighted that accurate numerical simulations incorporating a soil compaction simulation and a hardening soil model have been established to be a powerful way to establish the distribution of strains along geogrids. Nevertheless, the current study measured and assessed pressure distribution in the geogrids inside the best-built GRCS using a condensed numerical simulation [10]. The application of Geo-synthetic Reinforced Concrete Structures (GRCS) has shown appreciable prospects in improving the capacity of infrastructural systems exposed to static and/or dynamic loads. Nonetheless, ASR is still underutilized in areas sensitive to scour or other problems because of its apparent simplicity and relatively low cost. Previous work has mainly addressed reducing the drying shrinkage of pavements or improving the tensile properties with geogrids, and there is an acute knowledge gap in presenting and evaluating the strain distribution and load bearing capacity of GRCS under real application conditions, especially due to complex loads like earthquake or flood. Against this backdrop, this research seeks to fill these gaps by studying the behaviour of GRCS constructed near water sources. One of the main issues is related to the relatively low capacities of GRCS to resist scour-induced failures and the subsequent need to employ expensive protection measures.

However, there are few investigations on maximum offsets or other creative orientations in material configuration to minimize such risks without sacrificing cost implications. In addition, although Biaxial Geogrids (BG) have been analyzed in the laboratory, their effectiveness in replacing conventional reinforcement with steel to enhance ductility and seismic behavior has not been over-verified. The current study, therefore, seeks to address this by carrying out experimental and numerical analysis to assess the structural and cost-effective tendency of the GRCS with geogrid reinforcement. More precisely, this paper focuses on investigating strain fields in geogrids during the construction and service stages and on comparing the outcomes of the experiments with the results obtained through the FEM analysis to identify suitable design solutions in terms of the initial cost and structural performance under environmental disturbances.

2. Related Work

The usage of geogrids influences concrete pavement with drying shrinkage behavior. After being cleaned and cured for a week, two distinct sorts of specimens were stored for fifty-six days in a drying room [11-12]. The first compass was created of 75 mm-thick concrete prisms. Furthermore, certain specimens served as controls, and others discussed a single biaxial geogrid sheet at two different altitudes. The test outcomes demonstrate that the drying shrinkage strain may be reduced from 0.7 to 15% when geogrid supplements are compared to unreinforced prisms [13].

In contrast, geogrid sheets positioned 20 mm from the top significantly reduced the drying shrinkage strains throughout the initial phases better than those at 37.5 mm. Two virtually identical groups (positioned at 20 and 37.5 mm) showed nearly the same effects after 21 days [14-15]. The remaining illustrations comprised concrete slabs with an average thickness of thirty meters. It demonstrated that a mixture of geogrid and concrete reinforced with steel fibers (SFRC) substantially enhanced the properties of the samples. It was followed by the indication that geogrid confinement, with or without steel fibers, was the preferred option for objects that are cylinders under split tension [16].

Geo-synthetics have been used for decades to stabilize soils and enhance infrastructure performance. The shifted set was initiated from geotextiles in place and transformed to geogrids used in pavements and retaining structures. Bathurst et al. 1993 introduced most of the key concepts on geogrid behavior in soil due to the importance of geogrid soil in providing tensile resistance. This technology is most suitable when used in structural reinforcement applications.

Several studies on geogrids have shown that they can substitute steel reinforcements, especially in areas that require minimum weight and cost. Recent work by Majumder and Saha (2021) focuses on the enhancement of geogrid towards the RC beam-column joints and the enhancement of their ductility as well as their seismic performance. Specifically, with regard to load distribution benefits, Huang et al. (2015) discussed geosynthetic-reinforced soils in channel crossings. However, these concepts have not been developed with high fidelity in full-scale applications under different load cases, such as earthquakes and/ or soft soils. Finite Element Methods (FEM) have emerged as the standard tool needed to analyze geosynthetic-reinforced structures. Taha et al. (2014) identified and validated the use of FEM to estimate effective pile-reinforced systems based on experimental data available. Hwang and Juang (2013) presented a method for simulating differential settlement effects on geosynthetic-reinforced retaining walls. However, these models often do not include data corresponding to the structure's actual use, so the gaps in strain distribution remain under static and dynamic applied load. The cost efficiency of GRCS is a major research interest. The most recent studies by Nasiri and Hajiazizi in the summer of 2021 proved cost reduction in a geosynthetics technique for slope stabilization. However, many detailed cost structures that encompass long-term durability and reliability for the structures are lacking.

Tests on flexural beams showed that because geogrid functioned as a practical fracture bridging mechanism, the quantity and strength of geogrid sheets were important in improving load-deformation behavior and preventing crack propagation. [17-18]. The behavior of specimens under periodic stress in geogrid and conventional confinement, with and without SFRC, at the beam-column joint. [19-20].

2.1. Research Gap

While the benefits of geogrids in improving structural performance are well-documented, significant gaps remain:

- Some GRCS tests applicable environment conditions upon different landscape types do not enjoy broad real-world certification.
- Lack of adequate consideration of seismic performance and distribution of strain throughout the development phases.
- This is especially because of inadequate detailed cost and environmental appraisals of the proposal.

These gaps are expected to be addressed in this study by combining computed and experimental data on strain behavior and GRCS cost efficiency and assessing possible practical applications.

3. Material Properties

3.1. Concrete Material

For each sample, one batch of ready-mix (R/M) concrete was used for building. The principal parts of the substantial included sand, Type I Portland concrete, and exactly evaluated coarse total with the greatest size of 9.5 mm. The ACI 211.1-91 (2009) has been embraced to decide the extent of the blend plan. By changing the water-to-cement proportion, it was feasible to accomplish a strength.

3.2. Foundation Soil

The site foundation soil is constructed of low-plasticity clay (CL) with a diameter of about nine meters deep. Table 1 displays the physical characteristics that are that are near the bottom of the GRCS. Direct shear tests were completed to determine the foundation soil's effective shear strength (Table 1). However, this depth changed proportionately to the river's water level. The average measurement regarding the bottom of the BA is the insufficient shear force cu = 60 kPa, the pedometric modulus Eoed = 1900 kPa, the compression index Cc = 0.1663, and the swelling index Cs = 0.0198.

3.3. Geogrid

The mechanical and physical qualities of geogrids substantially impact the confining mechanism's effectiveness. In other words, the attributes of geogrids affect their performance. As apparent in Figure 1, Biaxial Geogrids (BG) provide ductile support both transversally and longitudinally.

Table 1. The features of foundation soil

Soil Classification and Depth CL	Water Content w (%)	Liquid Limit w_L (%)	Plastic Limit W_P (%)	Natural Density (ρ) Mg/m^3	Dry Density (ρs) Mg/m^3
3.0-3.4 mm	25.87	28.48	17.35	1.93	1.55
3.6-3.8 mm	30.87	34.98	21.56	1.56	1.48
3.9-4.2 mm	32.57	41.39	24.65	1.87	1.37

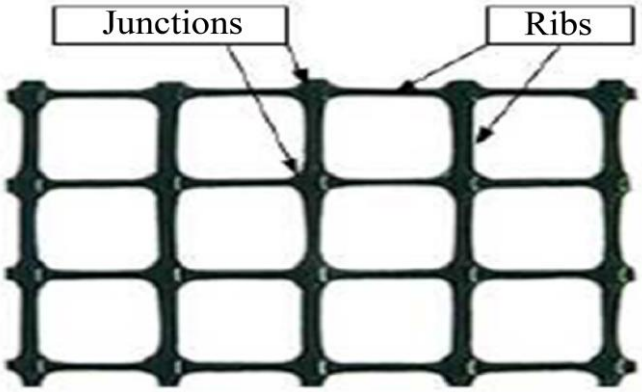

Fig. 1 Geogrids are biaxial plane layer

Table 2. The Biaxial Geogrids (BG) mechanical and physical features

Property	Unit	Value
Load at 3% deformation	KN/m	15
Load at 5% deformation	KN/m	29
Maximum tensile strength (L/T)	KN/m	40/40
Aperture dimensions (L/T)	mm/mm	34/34
Rib Width dimension (L/T)	mm/mm	2.3/2.5
Rib thickness dimension (L/T)	mm/mm	2.3/1.5

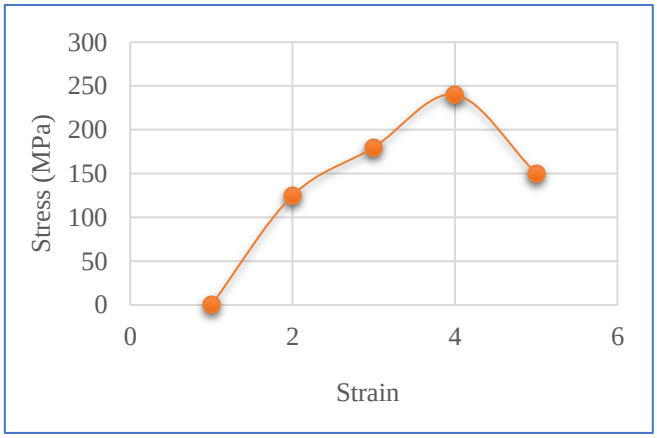

Fig. 2 Prime instance of the biaxial geogrids' (BG) stress-strain curve

They are made up of two-directional, thin ribs connected at denser joints. The non-woven stiff geogrids used in the current study were punched-drawn geogrids composed of high-density polypropylene. The supplier requirements for the geogrids are presented in Table 2, and a simulation of the stress-strain curve in Figure 2.

3.4. Fill Material

In the specific case, according to consideration. This is the fill material that was composed of gravel. When the gravel is exhibited, it very well may be classified as less than poor grade level (GP) utilizing a coefficient of bending (Ccu) of 3 and a level of homogeneity esteem (Cu) of 18. The fill material's grain size dispersion is the solids having a 2.84 mg/m3 density. The fill soil's most effective moisture content of 6.8% and the biggest dry unit weight of 21.48 kN/m3 have been identified by a modified Proctor test. A 2 mm sieve was used to determine the effective angle of shearing resistance, which measured out to be 45°.

3.5. Sample Preparation

The concrete samples were prepared as 75 mm-thick slabs and 230 mm-high columns for brick-mortar-interlayer and cement-mortar-interlayer. The geogrids were placed at specific heights in the specimens. Samples were treated under burlap for 14 days and air-dried to provide further sample preparation for subsequent tests. In order to ensure consistency, constant curing conditions were used throughout the experiment.

3.6. Experimental Setup

A Tinius Olsen universal testing machine was employed for axial and flexural load tests. The capacity and accuracy of the machine were set before the experiment was conducted.

Strain Gauges are attached to geogrids to record pull out forces during loading. The axial and lateral displacements were captured using four linear variable displacement transformers placed appropriately. Integrated to monitor the applied load with the accuracy of ± 0.1 kN.

3.7. Testing Procedure

The measured load increased at 1.0 mm/min until the sample failed. Displacements were recorded at different points along the height of the specimen. Conducted on beam specimens with geogrids located at various heights. The sizes of load and span met ASTM C78 specifications. Proctor compaction tests were conducted to identify the optimum moisture content and the dry unit weight.

3.8. Measurement Techniques

Details of the force exerted on the specimens and their deformation were recorded using strain gauges and LVDTs connected to an integrated data acquisition system with a sampling rate of 10Hz. All the calibration was done before each test was conducted. The forces applied in the geogrids were computed through the stress versus strain relationships derived from the geogrid material characterization tests.

3.9. Sample Size and Repetition

A total of 30 specimens were tested, including variations in the Presence and extension of geogrid layers, where it can be single or double layers. Several geogrid layers are within the specimen: Top, middle, third, and bottom. The stiffness of foundation soil is a three-tier variation. The above test configurations were performed thrice to get an overall average, which would reduce individual test variability.

4. Formwork Shape and Material Preparation

The specimens were allowed to air out under the age of drenched burlap for the final 14 days after getting cast, after being removed that extends from the formwork. The concrete had been merged employing an electric vibrator, intending for a 200 mm slump. All specimens displayed no signs of honeycombing after the forms were stripped. To keep the specimens moist after casting, wet burlap was thrown over each one.

4.1. Instrumentations and Testing

Fig. 3 Test set-up

The sample tests for removal control were completed on the usually realized Tinius Olsen testing machine. The samples were dislodged at a steady, typical uprooting pace of 1.0 mm/min until disappointment. Four Linear Variable Displacement Transducers (LVDTs) were utilized to estimate the typical axial deformations. They fitted the transducers along the focal point of the examples and joined sensors at the two finishes to get a gauge length of 230 mm. Two LVDTs were likewise situated between the actuator head and helped design to quantify pivotal disfigurements over the entire width of the example, with a gauge length of 500 mm. Every single important boundary, for example, loads applied on the sample and LVDT values, were recorded by an incorporated information assortment framework.

5. Results of Experimental Tests

The curve demonstrated in Figure 4 was utilized to translate the stresses discovered in the geogrids into forces. The abscissa axis reveals that the geogrid's overall length was 2.2 m. Over 55% of the total strain created during building the structure can be expressed by the curves that indicate forces in the geogrids at different stages of development.

Fig. 4 Adding reinforcement for the in-situ slab

As the loading was applied to the concrete specimens, thin longitudinal divisions on their outside began to demonstrate evidence of damage; these cracks subsequently grew and transmitted into the core region, accompanied by a series of loud noises caused by the rupture of the geogrid cartilage in joints. When the system finally was unsuccessful, the bulk of the concrete cover was ripping off, and the geogrid sheet had lost its anchor.

Ten working days following that, the manufactured beams were put in GRCS and commenced construction. The force in geogrid grew to 0.23 kN/m throughout that time, or around 12% of the total force that had previously developed.

The precast beam placement produced a 0.17 kN/ increase in strain, as demonstrated through Geogrid II. The geogrid's greatest tension, measured at 0.14%, was considerably smaller than the maximum strain identified in the other, which occurred at practically the same position (level 14, following surface loading).

5.1. Importance of Geogrid Layer Density

The specimens' axial load against the axial displacement graph illustrates the way the amounts of BG-50-1L, BG-50-2L, and unconfined geogrid layer changes, with a constant D/L ratio in Figure 5. Commencing at approximately seventy percent of the final load, there is a linear component of the load-displacement characteristic. Table 3 highlights the experiment's accomplishments.

Table 3. Test results

Specimen ID	Ultimate Load (KN)	Ratio of Ultimate Load α *	δy ** (mm)	δf ** (mm)	Displacement Ductility Index ($\mu+$)	Fracture Energy (N-m)	Energy Ductility Index (K ++)
C*	465.87	1.000	1.345	9.34	3.245	1364.45	1
BG-50-1L*	498.68	0.985	1.359	4.35	5.876	3345.98	2.345
BG-50-2L*	423.54	0.876	0.872	4.87	6.543	3675.35	2.434
BG-40-1L*	498.11	1.023	1.926	5.92	8.454	3985.25	2.547
BG-45-1L*	467.98	0.982	1.985	6.98	5.365	4876.34	2.765
BG-55-1L*	436.91	1.913	1.323	5.32	6.646	3875.65	1.564
S-50-5	547.76	1.578	0.864	8.35	9.54	3546.65	2.464

(a) (b) (c)

Fig. 5 Test set-up Typical failures: (a) BG-40-1L, (b) BG-45-1L, and (c) BG-55-1L

Figure 6 illustrates the impact of varying the total number of biaxial geogrid layers on the load-displacement response. Compared to the maximum load achieved by the unrestricted control specimen, a 1% enhancement was observed in the specimen with a single Biaxial Geogrid (BG) layer. The specimen with two BG layers exhibited an approximate 7% increase. Figure 7 depicts the Ductility Index (μ), determined by the proportion of axial displacements, indicating the structure's capacity for re-distribution.

5.2. Computation of the Final Portions of the Geosynthetic-Reinforced Concrete Structure

The GRCS's FE Model (FEM) was developed, and its loading performance was reviewed. FE Phase 2 software was deployed to model the GRCS. An FE mesh with 3202 nodes and 5220 elements has been generated. Triangles with three nodes have been employed to create a graded mesh. For the geogrid, a horizontal elastic, entirely plastic model was employed. Structural interfaces that enabled sliding between the geotextile and the fill material were employed to form the geogrid layers. Utilizing the Mohr-Coulomb slip criterion, the plastic slip was evaluated. Repairing the proper balance of the foundation soil layer was the initial and most significant process. In stage 2, the pit's excavation was completed. Phases 3–12 included creating the BA Stage 13 included modelling the precast bridging girder assembly (L1a) with a load of 75 kPa. As a result, Stage 14 employs the top of the concrete in situ slab with a load of 230 kPa (L2a). Features of Stage 15.

Although only two geogrids at differing degrees of highlights were tested, only at those two levels is it conceivable to contrast the geogrids' measured induced load employing the FEM. Figure 8 displays the induced forces within each geogrid that were determined using the FEM. The results demonstrate that almost all of the geogrids provided loads of 0.8 kN/m to 3 kN/m at the final stage of the bridge structure's construction, which is commensurate with the previously measured information.

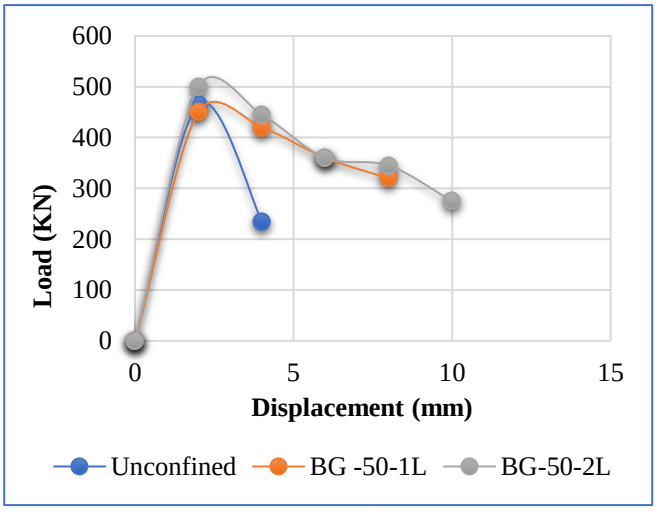

Fig. 6 Biaxial geogrid layer count's influence on load-displacement history

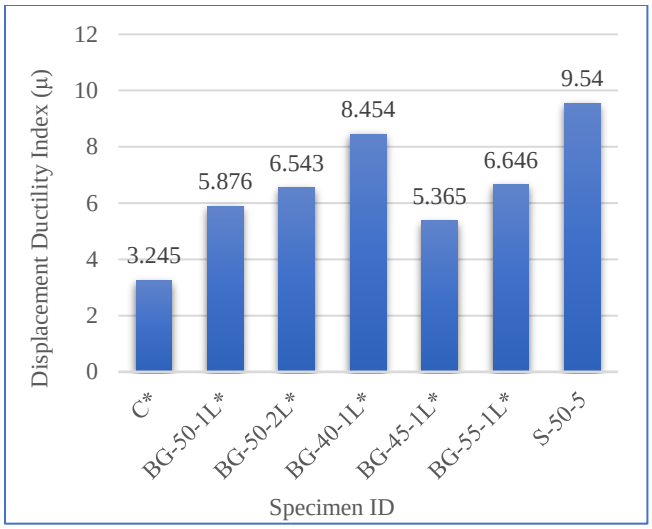

Fig. 7 Change in location estimated by a proportion of axial displacements, the ductility index (μ)

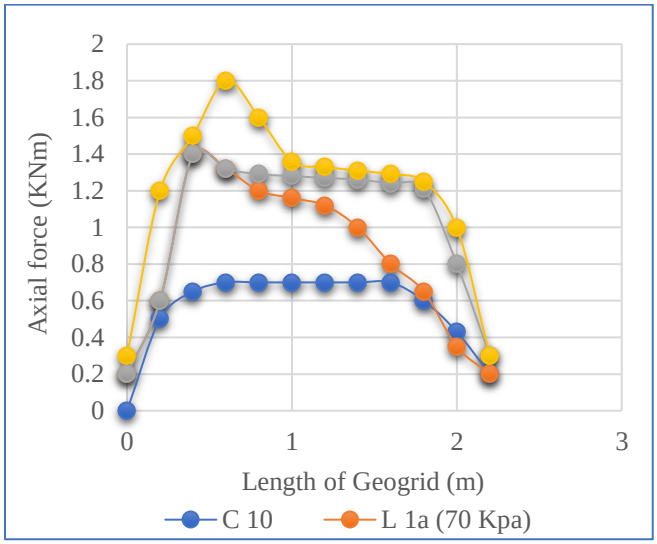

Fig. 8 Forces created along the geogrid that the FEM report

6. Numerical Modelling

The numerical modelling process of this study used FEM through FE Phase 2 software in order to analyse the strain and stress patterns in addition to load-bearing capacities in Geosynthetic Reinforced Concrete Structures (GRCS). A 2D plane model was realized using a graded triangular mesh that models the foundation soil with a Mohr-Coulomb criterion, concrete as elastic-perfectly plastic, and geogrids as linear-elastic elements: simulated real-life boundary conditions and incremental static and dynamic loads with appropriate seismic influence. The model was validated by comparing it with experimental data and previously published literature, with a deviation of less than 5% found. The simulation highlighted stress concentration zones, strain behavior, and optimized load-bearing capacities of the GRCS, thus highlighting the benefits of using numerical modelling for enhancing design and performance.

7. Long-term Performance and Durability

Geo-synthetic Reinforced Concrete Structures (GRCS) include environmental exposure, material properties, and structural design. Geo-synthetics, biaxial geogrids, for example, are made usually from polypropylene or polyester that are proven to resist environmental degradation, such as UV exposure, chemical attack, and biological activity. However, prolonged exposure to extreme conditions of high salinity, freeze-thaw cycles, and sustained UV radiation can lead to gradual material weakening. Protective measures, such as burying geogrids below the surface or using UV-resistant coatings, enhance durability. Furthermore, the redundancy in GRCS designs helps prevent localized failure, ensuring the structures remain stable for decades. With proper material selection and protection, studies show that GRCS can be used for over 50 years, making them sustainable long-term infrastructure.

8. Conclusion

This study outlines the comprehensive methodology for constructing a Geosynthetic Reinforced Concrete Structure (GRCS), including geogrid installation and strain monitoring. It was observed that soil compaction accounted for more than half of the strain sustained during construction. The geogrid's maximum load-bearing capacity was 3 kN/m, which is significantly lower than the material's tensile strength. The stress distribution was concentrated beneath the sill and exhibited an irregular pattern along the geogrid. A Finite Element Method (FEM) analysis effectively predicted the strain behavior in the reinforcement layers. The correlation between measured strains and FEM values confirmed that soil compaction greatly influences strain development in geogrids. Cost analysis revealed that GRCS constitutes only about 25% of the total construction cost for small-scale structures. By replacing traditional reinforced concrete abutments with GRCS, the overall construction expenditure can be reduced by up to 50%. An optimally designed GRCS can be up to four times more cost-effective than conventional reinforced concrete structures. Furthermore, the flexibility of Basalt Matrix (BG) restricted examples with changing measurement to-level proportions was surveyed utilizing the energy pliability record (K) (going from 2.302 to 3.558) and the ductility index (going from 6.725 to 9.022), the two of which were fundamentally higher contrasted with examples without imprisonment. This study recognizes certain limitations, primarily laboratory conditions, which by their controlled nature cannot mimic real-world complexity and complexity, the type of geogrid that it focused on, and the exclusion of long-term degradation under extreme exposure to aggressive chemicals or sustained seismic activities. Within these limitations, however, the results show that GRCS can accomplish better ductility, cost reduction, and seismic resilience. Future research should focus on alternate geosynthetic materials, long-term in situ monitoring in various environments, and integration with more advanced modelling techniques to further optimize GRCS applications. The results provide a strong foundation for adopting GRCS in cost-effective, sustainable infrastructure projects, especially in high-risk regions.

Acknowledgments

The supervisor provided invaluable direction and unflinching support throughout this research, for which the author is very grateful.

References

[1] Jie Huang et al., "Experimental and Numerical Study of Geosynthetic Reinforced Soil Over a Channel," *Geotextiles and Geomembranes*, vol. 43, no. 5, pp. 382-392, 2015. [CrossRef] [Google Scholar] [Publisher Link]

[2] A. Taha, M.H.El Naggar, and A. Turan, "Experimental and Numerical Study on Lateral Behaviour of Geosynthetic-Reinforced Pile Foundation System," *Geosynthetics International*, vol. 21, no. 6, pp. 352-363, 2014. [CrossRef] [Google Scholar] [Publisher Link]

[3] Anas Daou et al., "Experimental and Numerical Investigations of Reinforced Concrete Columns Confined Internally with Biaxial Geogrids," *Construction and Building Materials*, vol. 263, 2020. [CrossRef] [Google Scholar] [Publisher Link]

[4] Rashad Alsirawan, Ammar Alnmr, and Edina Koch, "Experimental and Numerical Investigation of Geosynthetic-Reinforced Pile-Supported Embankments for Loose Sandy Soils," *Buildings*, vol. 13, no. 9, pp. 1-20, 2023. [CrossRef] [Google Scholar] [Publisher Link]

[5] Subhrasmita Majumder, and Showmen Saha, "Experimental and Numerical Investigation on Cyclic Behaviour of RC Beam Column Joints Reinforced with Geogrid Material," *Materials Today: Proceedings*, vol. 38, pp. 2316-2324, 2021. [CrossRef] [Google Scholar] [Publisher Link]

[6] M. Abdesssemed, S. Kenai, and A. Bali, "Experimental and Numerical Analysis of the Behavior of an Airport Pavement Reinforced by Geogrids," *Construction and Building Materials*, vol. 94, pp. 547-554, 2015. [CrossRef] [Google Scholar] [Publisher Link]

[7] Youwei Xu et al., "Experimental and Numerical Studies of a Strip Footing on Geosynthetic-Reinforced Sand," *International Journal of Physical Modelling in Geotechnics*, vol. 20, no. 5, pp. 267-280, 2020. [CrossRef] [Google Scholar] [Publisher Link]

[8] Masoud Nasiri, and Mohammad Hajiazizi, "An Experimental and Numerical Investigation of Reinforced Slope Using Geotextile Encased Stone Column," *International Journal of Geotechnical Engineering*, vol. 15, no. 5, pp. 543-552, 2021. [CrossRef] [Google Scholar] [Publisher Link]

[9] Waqas Hassan et al., "Experimental Study on Shear Strength Behavior and Numerical Study on Geosynthetic-Reinforced Cohesive Soil Slope," *Innovative Infrastructure Solutions*, vol. 7, 2022. [CrossRef] [Google Scholar] [Publisher Link]

[10] Mahmoud Elshafey, Mohamed Elnaggar, and Ahmed Yehia Abdelaziz, "Numerical Investigation of Quay Walls Reinforced with Geosynthetic," *Alexandria Engineering Journal*, vol. 60, no. 2, pp. 2303-2313, 2021. [CrossRef] [Google Scholar] [Publisher Link]

[11] Madhu Sudan Negi, and S.K. Singh, "Experimental and Numerical Studies on Geotextile Reinforced Subgrade Soil," *International Journal of Geotechnical Engineering*, vol. 15, no. 9, pp. 1106-1117, 2021. [CrossRef] [Google Scholar] [Publisher Link]

[12] Nader Hataf, and Mehdi Sayadi, "Experimental and Numerical Study on the Bearing Capacity of Soils Reinforced using Geobags," *Journal of Building Engineering*, vol. 15, pp. 290-297, 2018. [CrossRef] [Google Scholar] [Publisher Link]

[13] Richard J. Bathurst, and Fahimeh M. Naftchali, "Geosynthetic Reinforcement Stiffness for Analytical and Numerical Modelling of Reinforced Soil Structures," *Geotextiles and Geomembranes*, vol. 49, no. 4, pp. 921-940, 2021. [CrossRef] [Google Scholar] [Publisher Link]

[14] Yewei Zheng, and Patrick J. Fox, "Numerical Investigation of Geosynthetic-Reinforced Soil Bridge Abutments Under Static Loading," *Journal of Geotechnical and Geoenvironmental Engineering*, vol. 142, no. 5, 2016. [CrossRef] [Google Scholar] [Publisher Link]

[15] O. Rahmouni et al., "A Numerical Investigation into the Behavior of Geosynthetic-reinforced Soil Segmental Retaining Walls," *International Journal of Geotechnical Engineering*, vol. 10, no. 5, pp. 435-444, 2016. [CrossRef] [Google Scholar] [Publisher Link]

[16] Liang Lu et al., "Experimental Study of the Performance of Geosynthetics-reinforced Soil Walls under Differential Settlements," *Geotextiles and Geomembranes*, vol. 49, no. 1, pp. 97-108, 2021. [CrossRef] [Google Scholar] [Publisher Link]

[17] Hasthi Venkateswarlu, K.N. Ujjawal, and A. Hegde, "Laboratory and Numerical Investigation of Machine Foundations Reinforced with Geogrids and Geocells," *Geotextiles and Geomembranes*, vol. 46, no. 6, pp. 882-896, 2018. [CrossRef] [Google Scholar] [Publisher Link]

[18] Panpan Shen et al., "Two and Three-Dimensional Numerical Analyses of Geosynthetic-Reinforced Soil (GRS) Piers," *Geotextiles and Geomembranes*, vol. 47, no. 3, pp. 352-368, 2019. [CrossRef] [Google Scholar] [Publisher Link]

[19] Tuan A. Pham, and Daniel Dias, "3D Numerical Study of the Performance of Geosynthetic-Reinforced and Pile-Supported Emban006Bments," *Soils and Foundations*, vol. 61, no. 5, pp. 1319-1342, 2021. [CrossRef] [Google Scholar] [Publisher Link]

[20] Hayssam Itani, George Saad, and Ghassan Chehab, "The Use of Geogrid Reinforcement for Enhancing the Performance of Concrete Overlays: An Experimental and Numerical Assessment," *Construction and Building Materials*, vol. 124, pp. 826-837, 2016. [CrossRef] [Google Scholar] [Publisher Link]